

Contents lists available at ScienceDirect

Vision Research

journal homepage: www.elsevier.com/locate/visres



Psychophysics of neon color spreading: Chromatic and temporal factors are not limiting



Jingyi He^a, Ennio Mingolla^b, Rhea T. Eskew Jr. a,*

- a Department of Psychology, College of Science, Northeastern University, Boston, MA, USA
- ^b Communication Sciences and Disorders, Bouvé College of Health Sciences, Northeastern University, Boston, MA, USA

ARTICLE INFO

Keywords: Neon color spreading Color filling-in Modulation transfer function Contrast sensitivity function

ABSTRACT

Neon color spreading (NCS) is an illusory color phenomenon that provides a dramatic example of surface completion and filling-in. Numerous studies have varied both spatial and temporal aspects of the neon-generating stimulus to explore variations in the strength of the effect. Here, we take a novel, parametric, low-level psychophysical approach to studying NCS in two experiments. In Experiment 1, we test the ability of both cone-isolating and equiluminant stimuli to generate neon color spreading for both increments and decrements in cone modulations. As expected, sensitivity was low to S(hort-wavelength) cone stimuli due to their poor spatial resolution, but sensitivity was similar for the other color directions. We show that when these differences in detection sensitivity are accounted for, the particular cone type, and the polarity (increment or decrement), make little difference in generating neon color spreading, with NCS visible at about twice detection threshold level in all cases. In Experiment 2, we use L-cone flicker modulations (reddish and greenish excursions around grey) to study sensitivity to NCS as a function of temporal frequency from 0.5 to 8 Hz. After accounting for detectability, the temporal contrast sensitivity functions for NCS are approximately constant or even increase over the studied frequency range. Therefore there is no evidence in this study that the processes underlying NCS are slower than the low-level processes of simple flicker detection. These results point to relatively fast mechanisms, not slow diffusion processes, as the substrate for NCS.

1. Introduction

1.1. Neon color spreading illusion

Perceived colors are a result of complex spatial and temporal interactions of multi-staged neural processes. This study focuses on how spatially distributed contextual information that induces neon color perception from a stimulus that propagates over space *and* time. Neon color spreading (NCS) affords a unique opportunity to psychophysically probe aspects of such temporal factors, because small changes in display configurations can support or eliminate induced color spreading in static displays (Redies & Spillmann, 1981; see Fig. 1).

The appearance and strength of neon color spreading (NCS) can be affected by many factors (Bressan, Mingolla, Spillmann, & Watanabe, 1997). Such factors include certain spatial properties, such as collinearity, depth cues, transparency cues and coloration (Nakayama, Shimojo, & Ramachandran, 1990; Pinna, Porcheddu, & Deiana, 2018; Redies & Spillmann, 1981), as well as temporal factors. Redies and

Spillmann (1981) reported that the shortest presentation duration for inducing neon color spreading was about 30 ms, at which the effect was as strong as with longer viewing duration. They also reported that neon color spreading is enhanced by illuminating the entire stimulus by flickering light and maximized at 15 Hz, suggesting that a transient visual mechanism might be involved. Cicchini and Spillmann (2013) studied how stimulus onset asynchrony (SOA) and stimulus termination asynchrony (STA) for flashed NCS pattern affects perception of the neon effect. They used patterns with sustained black rays and a transient red star, and the reverse (sustained star & transient rays), with controlled duration of SOA and STA. The optimal condition for generating NCS was shown to be that when the rays and the star have the same onset or offset, especially the latter, with the combination of a transient star and sustained rays. They argued that the augmentation effect of transients might be due to increased visibility, likely with an origin early within the visual system, and that the rays and the star are temporally integrated via different mechanisms. They also reported that a longer duration of the transient stimulus improves the effect. These findings

E-mail address: r.eskew@northeastern.edu (R.T. Eskew).

^{*} Corresponding author.

together suggest that temporal properties influence neon effect strength, likely originating at early stages.

1.2. Current study

Our study addresses two questions. First, whether NCS strength varies with the color of the crosses, by measuring sensitivity to NCS as a multiple of detection threshold. We used physiologically important color directions defined by increment and decrement modulations of the cone photoreceptor types, plus equiluminant red and green.

The second question addressed by our study is whether the dynamics underlying neon color spreading are slower than non-illusory color perception. For example, diffusive filling-in is likely to be slow (Cohen-Duwek & Spitzer, 2019; Grossberg & Mingolla, 1985; Huang & Paradiso, 2008; Paradiso & Nakayama, 1991), and would limit the creation of neon percepts at higher temporal frequencies. On the other hand, other processes such as produced by multiscale filtering could produce effects similar to filling-in but occur quickly (e.g., Blakeslee, Cope, & McCourt, 2016; Blakeslee & McCourt, 2008, 2011; Dakin & Bex, 2003)— that is, generation of the illusory percept would not be temporally limiting beyond the effects of temporal frequency on simple detectability of the flicker.

The logic behind our approach to these two questions is as follows. We assume that whatever cortical process generates NCS is preceded by a stage or stages that assess the chromaticity of the crosses with either the steady or flickering stimuli. In other words, there is a serial dependence of NCS on determination of the hue of the crosses themselves. This assumption accords with the finding that neon only appears when the chromatic stimulus is above its detection threshold (Goda & Ejima, 1997). This dependence is also consistent with the hue of NCS being approximately the same as the hue of the inducing cross (Redies & Spillmann, 1981), rather than some other hue generated by some independent and parallel process. Within this general framework, we can use the basic detection results to factor out the low-level effects of chromaticity and temporal frequency, and ask what (if any) effects these factors have at the presumed later stage or stages generating NCS.

Experiment 1 tests possible differences in processing across chromatic axes. Redies and Spillmann (1981) varied the color of the background by use of Munsell papers, and found a strong effect of color. Ejima, Redies, Takahashi, and Akita (1984) reported that the strongest neon effect occurs when the star and the surrounding Ehrenstein figure are complementary colors while similar colors provide weak effects, likely because that the illusory neon color is an additive mixture of the segment color and the complementary of the lattice color (da Pos & Bressan, 2003).

In the present study we measure effects of using different chromatiticies, specifying them in terms of their cone photoreceptor responses. Sensitivity to stimuli with the crosses having increment (+) and decrement (-) L, M, S-cone contrasts, as well as equiluminant red (L+ and M-) and green (M+ and L-) color directions, were examined in both steady and flickering conditions. The increment and decrement

directions potentially isolate ON and OFF pathways, which have important physiological and perceptual differences (Dacey, 2000; Gabree, Shepard, & Eskew, 2018; Rider, Henning, Eskew, & Stockman, 2018; Schiller, 1992; Shi & Eskew, 2024; Wang, Richters, & Eskew, 2014), allowing us to test for differences that might be attributable to these parallel visual pathways.

The L-cone increment (L+) stimulus in our study is similar to commonly used conditions that contain a red cross, which consistently produce a vivid neon effect (Cicchini & Spillmann, 2013; Redies & Spillmann, 1981). One comparison of interest in the present study was to compare those chromatic directions that appear reddish with those that appear greenish. In addition to equiluminant red, the L+, M-, and S+ appear reddish, with the last being reddish-blue or purple in color. The greenish ones are the complements (equiluminant green, L-, M+, and S-), with the S- appearing a greenish yellow.

In Experiment 2, we parametrically characterize the dynamic properties of NCS by measuring the temporal contrast sensitivity function (tCSF) for sinusoidal modulations of luminance and color, over a range of temporal frequencies. Sensitivity for the hue of the crosses (real color) and the neon effect induced by the crosses (illusory color) were measured with the same stimulus. Differences between the two curves reflect differences in the timing of cortical processes between real color and illusory color processing.

Previous studies have shown that the NCS disappears with a slight rotation of the colored cross (Redies & Spillmann, 1981) relative to the orientation and position of the inducing black lines (Fig. 1c). The effect of spatial misalignment was also incorporated in this experiment with the addition of temporal modulations. With the local spreading effect broken by rotating the crosses relative to the black arms of the grid, sensitivity for the crosses themselves can be measured directly without intrusion of the spreading effect.

Under bright conditions, the achromatic tCSF curve has a band-pass shape, such that sensitivity is highest at intermediate frequencies and falls off below and above, whereas the chromatic tCSF curve has a low-pass shape, with sensitivities below a 'corner' or cut-off frequency being constant (Petrova, Henning, & Stockman, 2013; reviewed in Taveras-Cruz, He, & Eskew, 2022; Watson, 1986; Wuerger et al., 2020). Therefore, we expect the tCSF shape for detection of aligned and misaligned reddish crosses to be band-pass, because these are luminance modulations (with colored stimuli). Judgments of the hue of the crosses and neon effect are expected to be low-pass, as these are chromatic judgments.

2. General methods

2.1. Observers

Seven practiced observers with normal color vision and corrected-tonormal acuity participated in this study. Their color vision was verified by the Hardy-Rand-Rittler (HRR) color plates (4th Edition), and five of them were also screened by Farnsworth–Munsell 100 hue test. Informed

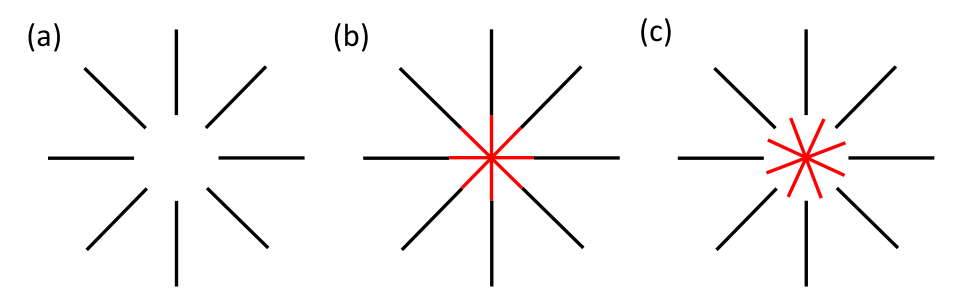


Fig. 1. Neon color spreading (NCS). (a) The Ehrenstein figure: the black radial pattern alone generates an illusory circular contour within which brightness is higher compared to surroundings. (b) When the colinear red star is added to the Ehrenstein figure, the red color seems to flow out and fill in the illusory contour, resulting in a diaphanous glowing red disk. (c) When the red lines and the black lines are non-colinear, NCS disappears (Redies & Spillmann, 1981).

consent was given by all observers, and experimental procedures in this study were approved by the Northeastern University Institutional Review Board and followed the Declaration of Helsinki.

2.2. Apparatus

Stimuli were presented on a Trinitron CRT monitor with an 85 Hz refresh rate, driven by a Macintosh computer together with a Bits# display controller (Cambridge Research Systems, Rochester, UK). The program was written using the Psychtoolbox (Kleiner, Brainard, & Pelli, 2007) in MATLAB (MathWorks, Natick, MA). The monitor was carefully calibrated. Gamma correction was performed by loading in a corrected color look-up table to the Bits#, which supports 14-bit intensity resolution; temporal frequency was confirmed with an oscilloscope connected to a fast photocell. The experiment was conducted in a dark room. The white (x = 0.283, y = 0.311) background luminance was 166 $\rm cd/m^2$, the maximum brightness of the monitor.

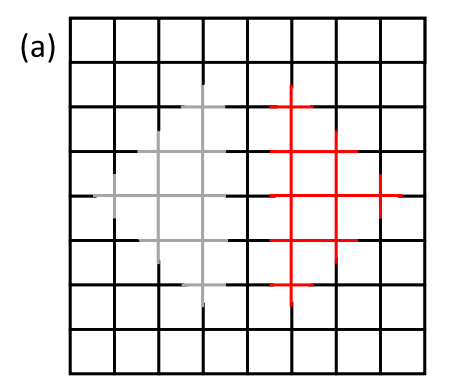
Observers' head position was fixed using a chin rest at a distance of 130 cm from the screen. The observers viewed the stimuli monocularly through ophthalmic trial lenses with their dominant eyes. Eye dominance was determined by a motor test (modified from the technique of Miles, 1930) prior to all other measures.

2.3. Stimuli

The stimulus consisted of an 8×8 (7.95 deg²) black grid with nine reference crosses and nine test crosses (Fig. 2). This grid was presented at the center of the screen on the uniform white background. The grid was black with the RGB channels set to zero.

Each cross within the grid subtended approximately 1 deg width and height. The reference side (left sides in Fig. 2) and the test side (right sides in Fig. 2) formed two triangles pointing left and right. The crosses within the reference side were gray (the same chromaticity as the white background but at half the luminance), and were not modulated. The test crosses were flickered symmetrically about the same mid-grey as the reference crosses. In a control condition used in Experiment 2, the crosses in the stimulus were no longer aligned with the background grid, but were rotated by 45° (Fig. 2b), but were otherwise the same as the aligned condition. This misalignment breaks the color spreading so that thresholds for modulations of the crosses themselves can be measured.

The chromaticities of the crosses were determined using the cone fundamentals of Stockman and Sharpe (Stockman & Sharpe, 2000; Stockman, Sharpe, & Fach, 1999). The spectral power distributions of the three monitor guns were measured using a PR-650 spectroradiometer. These distributions were cross-multiplied with the L-, M-, and Scone fundamentals to allow us to modulate particular cone types in isolation or combination, using standard silent-substitution methods (Estévez & Spekreijse, 1982; see He, Taveras-Cruz, & Eskew, 2021,



Appendix). The cone contrasts were computed relative to the mid-grey in the reference crosses, not relative to the white background, so that the mean chromaticities of the two sides of the stimulus match. Equiluminance was determined individually for each observer in experiment 1, using heterochromatic flicker photometry (at 10.63 Hz); the methods were the same as in He, Tayeras Cruz, and Eskew (2020).

3. Experiment 1: Chromatic effects

3.1. Stimuli and tasks

The aligned stimulus configuration was used in experiment 1 (Fig. 2a). Eight color directions (four symmetric pairs) were tested as color of the test crosses: S+, S-, M+, M-, L+, L-, equiluminant red and green. The stimuli were either steady or flickered at 1 Hz.

Seven observers participated in experiment 1. In the steady (non-flickering) condition, the contrast of the test cross was adjusted by the observer between white and fully saturated color (maximal cone contrast modulation with the indicated polarity, e.g., 0 to maximum available M+contrast). In the flicker condition, the test crosses sinusoidally flickered between one chromaticity and its symmetrical opposite direction in cone space (e.g., M– to M+), and the modulation depth of the flicker was varied by the observer. The mean of the flicker was the same as the gray reference crosses. Although two colors are alternated, participants were instructed to attend to only one of the two hues in each condition in making their threshold setting.

Three criteria were used for thresholds. The first criterion asked the observer to set the contrast at which the color of at least one test cross was just seen in the steady display (Task 1, steady color detection). With the second criterion, the observer set a threshold when just being able to see a large neon color triangle on the test side in the steady display (Task 2, steady neon detection). With the 1 Hz flickering stimuli, observers were asked to set thresholds for each color modulation polarity in separate runs (Task 3, 1 Hz neon detection). The stimulus was the same for the two symmetric chromaticities; it flickered at 1 Hz between the two chromaticities (e.g., M– and M+, greenish to reddish color). In one set of trials, observers attended to one polarity of the flicker (e.g., M+), and set the threshold to just seeing a greenish neon triangle; in the other condition (e.g., M–), observers attended to the other polarity and set the threshold to just seeing a reddish neon triangle.

All thresholds were measured with a method of adjustment (MOA) procedure: observers altered the modulation depth of the flicker by keypressing until the criterion was satisfied. Informal reports of stimulus appearance were also recorded. Each observer completed one run (5 settings per color direction) for the steady detection task, which was the easiest task for the observers, and two runs (10 settings per color direction) for the other two tasks.

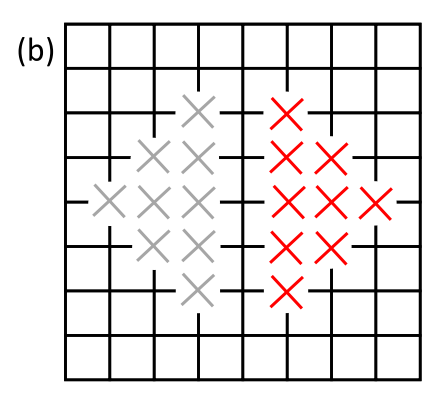


Fig. 2. Neon color spreading stimuli. Each stimulus contains two sides, one reference side in gray and one test side in red. The sides were randomly selected in the real experiment; in both panels here, the test side is on the right. (a) Aligned condition. All crosses (segments) are aligned with the grid to produce NCS. Three tasks/criteria were performed with this stimulus (see text). (b) Rotated condition. The crosses are rotated by 45°, and one task/criterion was measured with this stimulus.

3.2. Results and discussion

Mean flicker detection thresholds are shown in Fig. 3 as large blue triangles; each observer is plotted as a small orange triangle. Individual differences were minor. The S-cone detection thresholds are higher than the others, as expected, due in part to their low spatial and temporal resolution (Eskew, McLellan, & Giulianini, 1999; Smithson, 2014), but there is no clear evidence for sensitivity differences for the other color directions.

The mean neon color detection thresholds for steady and flickering stimuli are shown in Fig. 4 in multiples of chromatic detection threshold as a simple way to compare among color directions, adjusting for basic sensitivity differences. Observers were able to see steady or 1 Hz flickering neon color illusion at around 2–3 times the threshold for seeing color. In all color directions but S+, observers on average were slightly better at detecting 1 Hz flickering neon than steady neon (paired t-test: df = 7, p < 0.01). This finding agrees with previous evidence from Redies and Spillmann (1981) that the NCS illusion is enhanced by temporal modulation. Individual differences in seeing NCS were substantial, even after accounting for detection sensitivity.

Visual inspection of the data in Fig. 4 suggests that observers were slightly less sensitive in detecting neon produced by reddish colors (S+, M-, L+, equiluminant red) compared to greenish colors (S-, M+, L-, equiluminant green), even after chromatic sensitivity differences were accounted for. This difference was not statistically different from 0 for either the steady or flickering conditions (paired t-tests: df = 27, p = 0.58 and 0.77), but might be worthy of further study.

Most observers have similar sensitivity in each condition. Thus, the neon effect is approximately same for all tested color directions, in units of threshold multiples, with no within or between cone differences observed. No significant difference was found between equiluminant red and green neon colors and L-, M-cone colors, indicating that the neon effect is unaffected by the luminance of the colored stimulus.

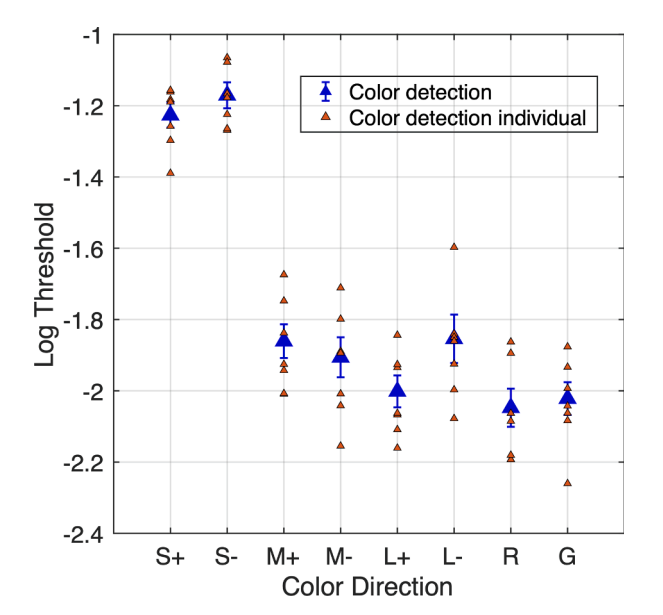


Fig. 3. Absolute detection thresholds. Mean cone contrast vector length thresholds for task 1 (flicker detection) for the eight color directions are represented by blue triangles. Error bars are \pm 1 standard error, based upon between-subject variability. The small orange triangles represent individual observer's mean thresholds.

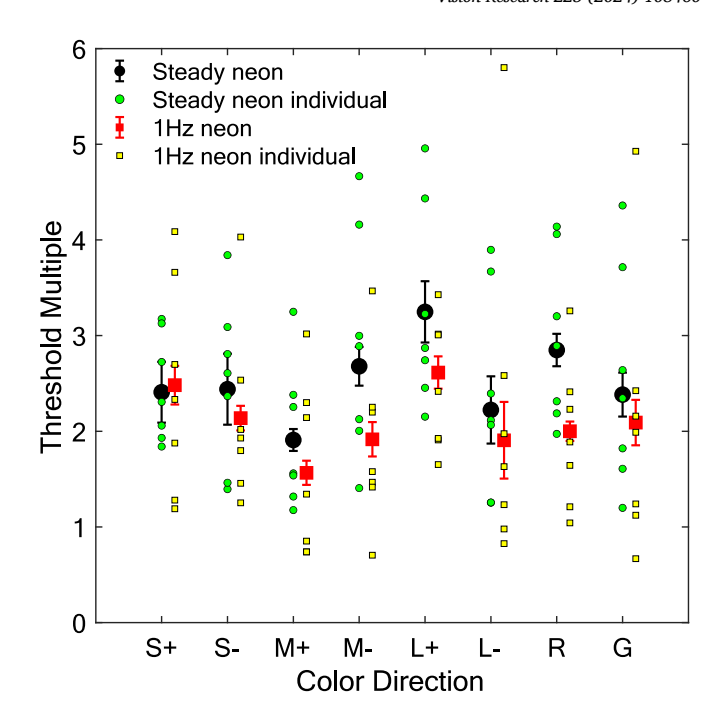


Fig. 4. Neon thresholds presented as multiples of flicker detection threshold. Black circles are mean steady neon threshold divided by mean steady detection threshold, while red squares are mean 1 Hz neon threshold divided by mean steady detection threshold. Error bars are \pm 1 standard error, based upon between-subject variability. Large symbols represent means over observers and small symbols are individual observers' mean settings.

4. Experiment 2: Temporal contrast sensitivity for neon color spreading

4.1. Stimuli and tasks

L- and M—cone modulations provide both chromatic and luminance signals, but for most observers, the luminance modulation produced by L cones is larger than that produced by M cones at the same cone contrast (by a factor of two, on average; He et al., 2020; Sharpe, Stockman, Jagla, & Jägle, 2011). L-cone modulations were used in Experiment 2 because their luminance component is likely to be a better stimulus for higher frequency flicker rates compared to some other colored stimuli. The test crosses sinusoidally flickered between L-cone increment (orange-red) and L-cone decrement (cyan) chromaticities.

The stimulus configuration in Fig. 2a was used for three measurements, based on three different criteria. For the first criterion, the observer was asked to select the contrast at which the flickering crosses are just seen to flicker, testing sensitivity to flicker of any cross using any perceptual cue (Task 1, aligned flicker detection) regardless of its color appearance. The second criterion measured sensitivity to the *hue* of the aligned crosses when observers were just able to see any color change in any flickering cross (Task 2, hue detection). With the third criterion, the observer made settings when just being able to see a flickering triangle on the test side (Task 3, neon color detection). With the aligned stimulus, NCS can be perceived because color of the crosses spreads out and fillsin the triangular region. A fourth measurement was based on the stimulus in Fig. 2b, testing sensitivity to the flickering crosses under conditions where no neon is present (Task 4, rotated flicker detection).

In all four tasks, the test crosses flickered sinusoidally at various rates. Six relatively low frequencies were adopted (0.5, 1, 2, 4, 6, 8 Hz) as chromatic sensitivity falls off quickly as frequency increases (Wuerger et al., 2020), and correspondingly the spectrally opponent parvocellular pathway prefers low frequencies (Lee, Pokorny, Smith, Martin, & Valberg, 1990).

The same method of adjustment procedure was used for all criteria.

Informal self-reports of stimulus appearance were recorded. Two runs (6 settings per frequency) were completed for each of the aligned condition, neon color condition, and rotated condition. One run (3 settings per TF) was completed for the hue condition. Three observers participated in experiment 2.

4.2. Results and discussion

Results are plotted as temporal contrast sensitivity functions (tCSF), reflecting how well the visual system follows the temporal modulation. Measured modulation sensitivities for the four tasks are shown in the top row in Fig. 5. The second row of the figure shows the modulation transfer functions (MTFs), based upon a simple linear systems model, fit to the data in the first row, as a way to smooth and interpolate the data. Details of the linear model fit are given in the Appendix (see *Linear Systems Model*). A fourth observer was excluded from this analysis because the data could not be fit using this modeling approach (data shown in Fig. A1), but the trend of the measured tCSFs was very similar to the other observers.

As demonstrated in Fig. 1, the rotated crosses are more visible than the aligned ones when steady. One would therefore reasonably assume that flicker sensitivity to rotated crosses might be higher than aligned

crosses, at least at low frequencies. However, surprisingly, two of our three observers are slightly more sensitive to aligned than rotated crosses with flicker (solid compared to dashed black curves, Fig. 5), even at the lowest temporal frequency measured (0.5 Hz). This might be due to the black lines providing a steady reference which the observer could use to judge the modulation of the colored line segments; this cue would be less available with the rotated crosses.

The hue curves are slightly lower than the (aligned) cross detection curves, indicating that chromatic sensitivity is somewhat lower than sensitivity to seeing any aspect of flicker (which might include, for example, luminance transients). The hue curves are very close to the rotated-cross curves, suggesting that the cross modulations were perceived (with any cue) with only slightly better sensitivity compared to color in the crosses (with the color cue). The hue curves (seeing color in the crosses themselves) are higher than the neon curves (seeing the illusory color), indicating that the strength of the induced color is weaker than the perception of the real color at all temporal frequencies. For all observers and all measured frequencies, sensitivity is higher for flickering crosses (in solid and dotted black) than for the neon illusion (in red), indicating that the neon effect is less visible than the flickering crosses that give rise to it. On average, sensitivity to neon is a factor of 2.5 (0.4 log units) lower than to the basic hue flicker (blue vs. red curves

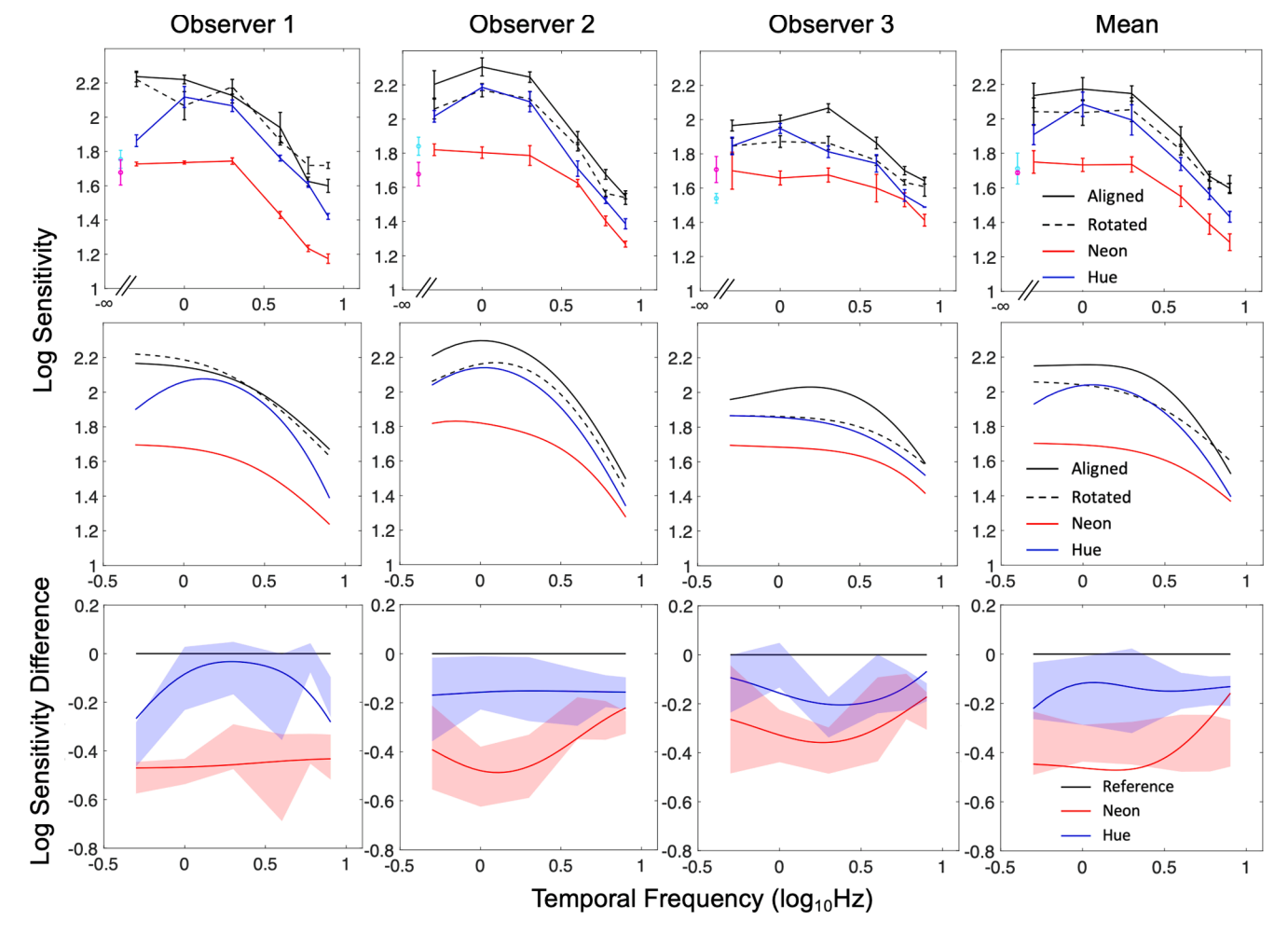


Fig. 5. Temporal contrast sensitivity functions (tCSFs) for L-cone crosses with the aligned detection task (solid black curve), the neon color task (red curve), rotated detection task (dotted black curve), and hue task (blue curve). The top row shows measured sensitivities. The magenta and cyan points in the individual panels in the top row correspond to sensitivities to steady neon stimulus (Fig. 2a) in L-cone increment (magenta) and L-cone decrement (cyan) color directions. The top row error bars show \pm one standard errors. The error bars for each observer indicate trial-by-trial variations whereas for the mean plot they depict between-subject variability. The middle row shows linear filter models fitted to the data. The bottom row shows differences between the aligned condition (black reference line) and another two tCSFs (hue and neon) in the middle row. The blue (hue) and red (neon) error bands indicate \pm 1.96 standard errors of the measured data (top row) around the mean of measured threshold differences, incorporating only between-subject variability.

in Fig. 5, top row).

The tCSF curves for the crosses, as well as 'hue', appear either as band-pass or low-pass shape, whereas the neon curves show a low-pass pattern, suggesting little or no temporal inhibition or adaptation for NCS (Watson, 1986). The magenta and cyan points in the top row of Fig. 5 represent sensitivities for the neon effect with a steady stimulus (for L+ and L-, respectively) tested in experiment 1. The two sensitivities are similar to or lower than the neon flicker curve, consistent with the slightly higher sensitivity for neon flicker compared to steady neon found in Experiment 1. According to the vertical position of the curves, the observers started to perceive the aligned stimulus in the order of detection (any cue), color cue in the crosses (real color), and neon color (illusory color) as contrast of the crosses increases. This order is consistent with observers' informal self-report. Although the observers differ in detail, the major features of the tCSF shapes, and the order of sensitivity to the different tasks, are the same for all observers.

The fitted model tCSFs are shown in the middle row in Fig. 5. The fitted functions show clear low-pass or band-pass shape. To better illustrate the relationship between the curves, differences between the aligned (solid black) and the other two curves are plotted in Fig. 5 bottom row. This analysis examines the effect of frequency on real and neon hue after accounting for the effect of flicker on detectability. The black line at zero sensitivity is the reference curve (the aligned condition curve, for flicker detection). The blue and red curves show the effect of temporal frequency on hue and neon judgments after the basic effect of flicker detectability has been factored out by taking the log difference. Confidence bands (± 1.96 standard errors), derived from the measured data in the top row of Fig. 5, for the hue (blue) and neon (red) difference curves are plotted as shaded regions. The curves are not centered within the confidence bands because the curves are calculated from the tCSF fit to the data, whereas the bands are calculated directly from the data themselves. The hue and neon curves are always below the reference line in the tested temporal frequency range. On average, sensitivity for seeing hue is more than 0.1 log units lower than the aligned (reference) condition, showing that the hue is perceived at a contrast that is more than 26 % higher than detection of flicker via any cue, with this method of adjustment procedure. For all individuals, sensitivity to neon is about 0.4 log units lower than the baseline temporal sensitivity at low temporal frequencies, and the difference changes only slightly with temporal frequency.

The question of greatest interest here is whether the temporal sensitivity to NCS shows evidence of slower processing (more temporal filtering) than flicker detection (in the aligned condition). If so, the red curves in Fig. 5 (bottom panels) should decrease as temporal frequency increases. There is no evidence that this happens; to the degree that there is any change in the red curves in the bottom row, they *increase* with temporal frequency, the opposite to the prediction of NCS being slower than detection. The confidence interval bands (Fig. 5 bottom row) based on the measured data points (not the fitted curves) show that the differences between neon and aligned curve decrease with frequency for Observers 2 and 3 while Observer 1 shows no change.

To analyze this question statistically, two repeated measures ANOVAs were performed using data from all four observers (including the data from the observer shown in the Appendix) to test the effect of temporal frequency. The ANOVA results were $F(5,15)=1.317,\ p=0.309,\ \eta_p^2=0.305$ for the neon difference and $F(5,15)=1.219,\ p=0.348,\ \eta_p^2=0.289$ for the hue difference. Thus the statistical analysis finds no significant effect of temporal frequency, consistent with both the hue (blue) and neon (red) sensitivities in the bottom row of Fig. 5 being effectively flat across temporal frequency. A post-hoc power analysis was conducted for the non-significant neon and hue difference conditions, yielding power values of 0.340 and 0.316, respectively, indicating low power levels. This is anticipated due to the limited number of observers. Given the low power levels, some caution is in order, but there is certainly no evidence in these results of an effect of temporal frequency

on hue or NCS after correcting for detectability.

Therefore, both neon and hue sensitivities either vary little or even increase with temporal frequency after accounting for the effect of frequency on detection. This result indicates that the dynamics of the mechanisms creating NCS do not limit or slow the perception of the illusion more than the dynamics of detection *per se*.

5. General discussion

Our two main findings are (a) that although our observers are less sensitive to some color directions (S+and S- compared to the others), as expected, once those differences in detection sensitivity are accounted-for there is no evidence of differences in sensitivity to NCS with chromatic direction; (b) analogously, there is little effect of temporal frequency on sensitivity for NCS, once the basic flicker sensitivity is accounted for.

In Experiment 1 we found that, at 1 Hz, neon color spreading persists in all tested color directions and produces better NCS than the steady condition, supporting a role for transient mechanisms in NCS (Cicchini & Spillmann, 2013; Redies & Spillmann, 1981). Neither steady or 1 Hz flicker conditions demonstrate clear cone-specific differences, indicating that there is no significant difference among color directions regarding the ability to produce neon effect after accounting for chromatic detection sensitivity. In addition, no significant difference was found between reddish and greenish colors. Our finding is consistent with previous evidence that good NCS can be obtained with various colors (Bressan et al., 1997). The effect produced by equiluminant colors are comparable to the commonly adopted red crosses that include a luminance modulation component, suggesting that equiluminance is not important in NCS. Once low-level chromatic sensitivity is equated, NCS does not vary with color direction.

The temporal contrast sensitivity functions for NCS provide evidence that sensitivity to the illusion per se does not differ much across temporal frequencies up to 8 Hz, relative to sensitivity to detection. There are no clear differences in shape of the sensitivity curves for neon compared to the shape of flicker sensitivity, except that the neon sensitivity curve is more of a low-pass shape. A slow color filling-in process, such as diffusion of color signals within a cortical area by electrochemical synapses, would predict a MTF pattern with the neon sensitivity decreases at higher temporal frequencies (after accounting for detection sensitivity). However, a decrease at high frequencies and temporal inhibition at low frequencies were not observed in our study, and there is no evidence that there are major delays in generating neon per se. Therefore, it can be presumed that either the limiting temporal process for NCS are early, or there exist rapid feedback projections from higher-level processing (Devinck & Knoblauch, 2019; Lamme, Super, & Spekreijse, 1998).

NCS is likely to be related to processing of figure/ground segregation and border ownership, as neon color is often contained in regions formed by illusory contours (Grossberg & Mingolla, 1985), such as the outlines of the illusory disks of Fig. 1. Layton, Mingolla, and Yazdanbakhsh (2012, 2014) analyzed how the physiological temporal factors of signaling between neurons involved in determination of borderownership constrain the types of cortical network that can plausibly underlie figure-ground segregation. Determination of border ownership for a "figure" region often requires some combination of relatively local and global information, as the connected outer contour of a figure region may meander over many degrees of visual angle. Studies of primate V2 have identified neurons whose response signals border ownership at local parts of a contour, so these neurons must also have access, directly or indirectly, to spatially remote (global) information confirming closure of a figure region's bounding contour (Qiu & von der Heydt, 2007; Zhou, Friedman, & von der Heydt, 2000). Such cells could access global information either intra-areally, i.e., by lateral unmyelinated connections within a single cortical area, such as V2, or interareally, i.e., where cells with larger receptive fields communicate contextual information about the scene via myelinated feedback projections to areas with smaller receptive fields that are fewer synapses away from the retina (Angelucci & Bullier, 2003; Angelucci et al., 2002). Intra-areal and interareal axonal conduction velocities have been estimated to be 0.3 m/s (Angelucci et al., 2002; Nowak & Bullier, 1997; Nowak, Munk, Girard, & Bullier, 1995) and 3.5 m/s in early visual areas, respectively (Bullier, 2001; Girard, Hupé, & Bullier, 2001). Interareal connections are thus an order of magnitude faster than intra-areal connections while spanning broad areas, and Layton et al. (2012, 2014) argue that these fast interareal connections are required to determine border ownership. We speculate that fast interareal processing underlies both "normal" and neon color processing and occurs at similar rates, consistent with our finding that there is no evidence in this study that the processes underlying NCS are slower than the low-level processes of simple flicker detection (Fig. 5).

How these network considerations may relate to multiscale filtering models (Blakeslee et al., 2016; Blakeslee & McCourt, 2008; Dakin & Bex, 2003) is beyond the scope of this paper. However, it is worth noting that the filtering models also account for at least many filling-in phenomena that are similar to NCS, and would not necessarily limit flicker sensitivity at high temporal frequencies, consistent with our results.

In summary, our results characterized chromatic variations and temporal dynamics of NCS with a parametric approach. We found no cone specific or color-specific differences and *no evidence for delayed temporal filtering for NCS*. These results are not consistent with slow, diffusive filling-in processes as the cause of NCS. It is likely that feedback processing is incorporated in illusory color processing. Relevant pathways are likely to be involved in the process of surface completion as well. The current study is a fundamental first step to parametrically describe temporal characteristics of the filling-in effect, putting effort to

bridging the gap between color physiology and psychophysics. Further examinations with a finer-scale perspective are needed to identify any specific neural substrate for NCS.

CRediT authorship contribution statement

Jingyi He: Writing – review & editing, Writing – original draft, Software, Investigation, Formal analysis, Data curation. Ennio Mingolla: Writing – review & editing, Formal analysis, Conceptualization. Rhea T. Eskew: Writing – review & editing, Supervision, Resources, Project administration, Funding acquisition, Formal analysis, Conceptualization.

Declaration of Competing Interest

The authors declare that they have no known competing financial interests or personal relationships that could have appeared to influence the work reported in this paper.

Data availability

Data will be made available on request.

Acknowledgements

Supported by NSF Grant BCS- 1921771. The authors thank Yesenia Taveras Cruz and Yangyi Shi for being observers. Current Address for Jingyi He is Herbert Wertheim School of Optometry and Vision Science, University of California Berkeley, Berkeley CA, USA.

Appendix

Linear systems model

A linear temporal filter model (Watson, 1986) was fit to these data to extract parameters characterizing each curve, as important aspects of the visual system can be revealed in the context of linear filters. Equations of the model are shown below:

$$|H_1(f)| = [(2\pi f\tau)^2 + 1]^{-\frac{n_1}{2}} \tag{A1}$$

$$|H_2(f)| = [(2\pi f \kappa \tau)^2 + 1]^{\frac{-n_2}{2}}$$
 (A2)

$$< H_1(f) = -n_1 \tan^{-1}(2\pi f \tau)$$
 (A3)

$$< H_2(f) = -n_2 \tan^{-1}(2\pi f \kappa \tau) \tag{A4}$$

$$|H| = \xi [|H_1|^2 + \zeta^2 |H_2|^2 - 2\zeta |H_1||H_2|\cos(\langle H_1 - \langle H_2 \rangle)]^{1/2}$$
(A5)

In the above equations, f denotes temporal frequency. The visual channel underlying detection of stimuli in Fig. 2 is considered as the difference of two low-pass filters, implying an excitatory mechanism and an inhibitory mechanism, with each consists of n identical low-pass stages. The parameter n, in part, controls the slope of the high-frequency limb of the MTF. Our analysis assumed that the two low-pass filters have the same number of stages for convenience. Time constants of the two filters are denoted by τ and $\kappa\tau$, respectively. κ can also affect the higher limb of the MTF curve. Two scaling factors are ξ and ζ . ξ adjust the overall response height. ζ determines the transience status of the model, with $\zeta=0$ indicating that only the excitatory mechanism remains as the low-pass filter, and with $\zeta=1$ indicating that the filter is transient as the band-pass filter. Therefore, Equation A1 and A2 represent the amplitude responses of the two filters, and Equation A3 and A4 denote their phase responses. The amplitude response of the combined filter is shown as Equation A5, which is the linear model used for fitting our MTF curves. Table A1 reports the best-fitting parameters for the linear filter model.

Table A1Best-fitting parameters of the linear filter model for each task for each observer.

Observer	#1				#2				#3				Mean			
Condition	Aligned	Rotated	Hue	Neon	Aligned	Rotated	Hue	Neon	Aligned	Rotated	Hue	Neon	Aligned	Rotated	Hue	Neon
n stages	1	1	3	1	2	2	2	2	2	1	1	2	2	1	2	1
τ (tau)	0.06	0.08	0.03	0.05	0.05	0.05	0.05	0.03	0.03	0.04	0.04	0.02	0.05	0.05	0.04	0.04
к (kappa)	2.10×10^{12}	1.30	3.95	1.30	3.85	2.78	3.57	10.65	3.49	1.25	1.32×10^{13}	116.62	1.33	1.30	4.58	9. 90×10^{11}
кт	1.27×10^{11}	0.10	0.11	0.07	0.19	0.13	0.18	0.33	0.10	0.05	5.25×10^{11}	2.16	0.06	0.07	0.18	3.81×10^{10}
ξ (xi)	149.21	170.63	119.79	50.36	238.12	203.61	172.26	63.84	127.21	135.96	73.98	48.79	322.52	115.65	123.04	50.76
ζ (zeta)	0.01	0.00	1.00	0.00	1.00	0.64	1.00	1.00	0.35	0.46	0.03	1.00	0.57	0.00	1.00	0.05
\mathbb{R}^2	0.77	0.69	0.93	0.87	0.88	0.85	0.95	0.87	0.80	0.58	0.82	0.32	0.97	0.95	0.98	0.89

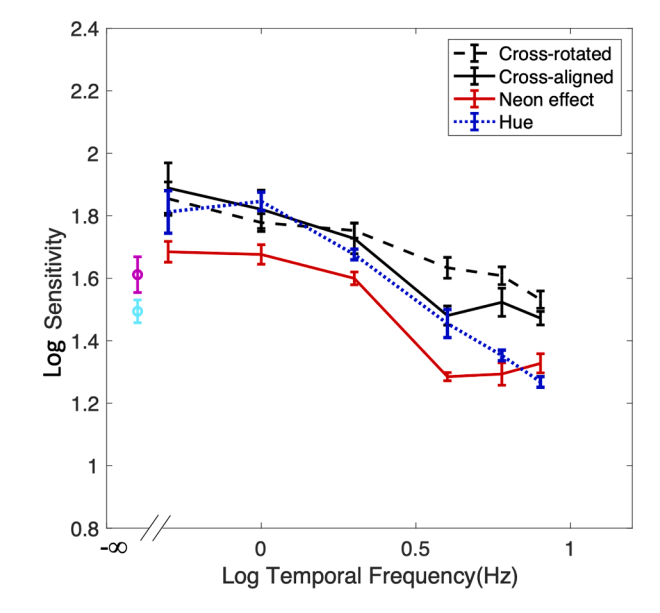


Fig. A1. Data of the observer excluded from linear systems modeling. The curves represent temporal contrast sensitivity functions (tCSFs) for L-cone crosses with the aligned detection task (solid black curve), the neon color task (red curve), rotated detection task (dotted black curve), and hue task (blue curve). The magenta and cyan points correspond to sensitivities to steady neon stimulus of this subject (Fig. 2a) in L-cone increment and L-cone decrement color directions, respectively.

References

Angelucci, A., & Bullier, J. (2003). Reaching beyond the classical receptive field of V1 neurons: Horizontal or feedback axons? *Journal of Physiology - Paris*, 97(2–3), 141–154. https://doi.org/10.1016/j.jphysparis.2003.09.001

Angelucci, A., Levitt, J. B., Walton, E. J., Hupe, J. M., Bullier, J., & Lund, J. S. (2002). Circuits for local and global signal integration in primary visual cortex. *Journal of Neuroscience*, 22(19), 8633–8646. https://doi.org/10.1523/JNEUROSCI.22-19-08632-2002

Blakeslee, B., Cope, D., & McCourt, M. E. (2016). The Oriented Difference of Gaussians (ODOG) model of brightness perception: Overview and executable Mathematica notebooks. *Behavior Research Methods*, 48(1), 306–312. https://doi.org/10.3758/ s13428-015-0573-4

Blakeslee, B., & McCourt, M. E. (2008). Nearly instantaneous brightness induction. Journal of Vision, 8(2), 11–18. https://doi.org/10.1167/8.2.15

Blakeslee, B., & McCourt, M. E. (2011). Spatiotemporal analysis of brightness induction. *Vision Research*, *51*(16), 1872–1879. https://doi.org/10.1016/j.visres.2011.06.018
Bressan, P., Mingolla, E., Spillmann, L., & Watanabe, T. (1997). Neon color spreading: A

review. *Perception*, 26(11), 1353–1366. https://doi.org/10.1068/p261353
Bullier, J. (2001). Integrated model of visual processing. *Brain Research Reviews*, 36(2–3), 96–107. https://doi.org/10.1016/s0165-0173(01)00085-6

Cicchini, M., & Spillmann, L. (2013). Neon color spreading in dynamic displays: Temporal factors. *Journal of vision*, 13(12), 2. https://doi.org/10.1167/13.12.2

Cohen-Duwek, H., & Spitzer, H. (2019). A compound computational model for filling-in processes triggered by edges: Watercolor illusions. Frontiers in Neuroscience, 13. https://doi.org/10.3389/fnins.2019.00225

da Pos, O., & Bressan, P. (2003). Chromatic induction in neon colour spreading. *Vision Research*, 43(6), 697–706. https://doi.org/10.1016/s0042-6989(03)00004-x

Dacey, D. M. (2000). Parallel pathways for spectral coding in primate retina. *Annual Review of Neuroscience*, 23, 743–775. https://doi.org/10.1146/annurev.neuro.23.1.743

Dakin, S. C., & Bex, P. J. (2003). Natural image statistics mediate brightness "filling in.". *Proceedings of the Royal Society of London. Series B: Biological Sciences, 270*(1531), 2341–2348. https://doi.org/10.1098/rspb.2003.2528

Devinck, F., & Knoblauch, K. (2019). Central mechanisms of perceptual filling-in. Current Opinion in Behavioral Sciences, 30, 135–140. https://doi.org/10.1016/j. cobeha.2019.08.003

Ejima, Y., Redies, C., Takahashi, S., & Akita, M. (1984). The neon color effect in the Ehrenstein pattern: Dependence on wavelength and illuminance. *Vision Research*, 24 (12), 1719–1726. https://doi.org/10.1016/0042-6989(84)90002-6

Eskew, R. T., Jr., McLellan, J. S., & Giulianini, F. (1999). Chromatic detection and discrimination. In K. R. Gegenfurtner, & L. T. Sharpe (Eds.), Color vision: From genes to perception (pp. 345–368). Cambridge, UK: Cambridge University Press.

Estévez, O., & Spekreijse, H. (1982). The "silent substitution" method in visual research. Vision research, 22(6), 681–691. https://doi.org/10.1016/0042-6989(82)90104-3

Gabree, S. H., Shepard, T. G., & Eskew, R. T., Jr. (2018). Asymmetric high-contrast masking in S cone increment and decrement pathways. Vision Research, 151, 61–68. https://doi.org/10.1016/j.visres.2017.06.017

Girard, P., Hupé, J., & Bullier, J. (2001). Feedforward and feedback connections between areas V1 and V2 of the monkey have similar rapid conduction velocities. *Journal of Neurophysiology*, 85(3), 1328–1331. https://doi.org/10.1152/jn.2001.85.3.1328

Goda, N., & Ejima, Y. (1997). Additive effect of luminance and color cues in generation of neon color spreading. *Vision Research*, *37*(3), 291–305. https://doi.org/10.1016/s0042.6989(96)00124-1

Grossberg, S., & Mingolla, E. (1985). Neural dynamics of form perception: Boundary completion, illusory figures, and neon color spreading. *Psychological Review*, 92(2), 173–211. https://doi.org/10.1037/0033-295X.92.2.173

He, J., Taveras Cruz, Y., & Eskew, R. T., Jr. (2020). Methods for determining equiluminance in terms of L/M cone ratios. *Journal of Vision*, 20(4), 22. https://doi. org/10.1167/joy.20.4.22

He, J., Taveras-Cruz, Y., & Eskew, R. T., Jr. (2021). Modeling individual variations in equiluminance settings. *Journal of Vision*, 21(7), 15. https://doi.org/10.1167/ joy.17.15

Huang, X., & Paradiso, M. A. (2008). V1 response timing and surface filling-in. *Journal of Neurophysiology*, 100(1), 539–547. https://doi.org/10.1152/jn.00997.2007

- Kleiner, M., Brainard, D. H., & Pelli, D. (2007). What's new in Psychtoolbox-3? Perception, 36(Suppl.), 14.
- Lamme, V. A., Super, H., & Spekreijse, H. (1998). Feedforward, horizontal, and feedback processing in the visual cortex. Current opinion in neurobiology, 8(4), 529–535. https://doi.org/10.1016/S0959-4388(98)80042-1
- Layton, O. W., Mingolla, E., & Yazdanbakhsh, A. (2012). Dynamic coding of borderownership in visual cortex. *Journal of Vision*, 12(13), 8. https://doi.org/10.1167/ 12.13.8
- Layton, O. W., Mingolla, E., & Yazdanbakhsh, A. (2014). Neural dynamics of feedforward and feedback processing in figure-ground segregation. Frontiers in Psychology, 5, 972. https://doi.org/10.3389/fpsyg.2014.00972
- Lee, B. B., Pokorny, J., Smith, V. C., Martin, P. R., & Valberg, A. (1990). Luminance and chromatic modulation sensitivity of macaque ganglion cells and human observers. *Journal of the Optical Society of America A*, 7(12), 2223–2236. https://doi.org/ 10.1364/josaa.7.002223
- Miles, W. R. (1930). Ocular dominance in human adults. The Journal of General Psychology, 3(3), 412–430. https://doi.org/10.1080/00221309.1930.9918218
- Nakayama, K., Shimojo, S., & Ramachandran, V. (1990). Transparency: Relation to depth, subjective contours, luminance, and neon color spreading. *Perception*, 19(4), 497–513. https://doi.org/10.1068/p190497
- Nowak, L. G., & Bullier, J. (1997). The timing of information transfer in the visual system. In K. L. S. Rockland, J. H. Kaas, & A. Peters (Eds.), Cerebral cortex: Vol. 12. Extrastriate cortex in primates (pp. 205–241). New York: Springer.
- Nowak, L. G., Munk, M. H., Girard, P., & Bullier, J. (1995). Visual latencies in areas V1 and V2 of the macaque monkey. Visual Neuroscience, 12(2), 371–384. https://doi.org/10.1017/s095252380000804x
- Paradiso, M. A., & Nakayama, K. (1991). Brightness perception and filling-in. Vision Research, 31(7–8), 1221–1236. https://doi.org/10.1016/0042-6989(91)90047-9
- Petrova, D., Henning, G. B., & Stockman, A. (2013). The temporal characteristics of the early and late stages of the L- and M-cone pathways that signal color. *Journal of Vision*, 13(4), 2. https://doi.org/10.1167/13.4.2
- Pinna, B., Porcheddu, D., & Deiana, K. (2018). Illusion and illusoriness of color and coloration. *Journal of Imaging*, 4(2), 30. https://doi.org/10.3390/jimaging4020030
- Qiu, F. T., & von der Heydt, R. (2007). Neural representation of transparent overlay. Nature Neuroscience, 10(3), 283–284. https://doi.org/10.1038/nn1853
- Redies, C., & Spillmann, L. (1981). The neon color effect in the Ehrenstein illusion. Perception, 10(6), 667–681. https://doi.org/10.1068/p100667

- Rider, A. T., Henning, G. B., Eskew, R. T., Jr., & Stockman, A. (2018). Harmonics added to a flickering light can upset the balance between ON and OFF pathways to produce illusory colors. Proceedings of the National Academy of Sciences of the United States of America, 115(17), E4081–E4090. https://doi.org/10.1073/pnas.1717356115
- Schiller, P. H. (1992). The ON and OFF channels of the visual system. Trends in Neurosciences, 15(3), 86–92. https://doi.org/10.1016/0166-2236(92)90017-3
- Sharpe, L. T., Stockman, A., Jagla, W., & Jägle, H. (2011). A luminous efficiency function, VD65*(λ), for daylight adaptation: A correction. Color Research and Application, 36(1), 42–46. https://doi.org/10.1002/col.20602
- Shi, Y., & Eskew, R. T., Jr (2024). Asymmetries between achromatic increments and decrements: Perceptual scales and discrimination thresholds. *Journal of Vision*, 24(4), 10. https://doi.org/10.1167/jov.24.4.10
- Smithson, H. E. (2014). S-cone psychophysics. Visual Neuroscience, 31(2), 211–225. https://doi.org/10.1017/S0952523814000030
- Stockman, A., & Sharpe, L. T. (2000). The spectral sensitivities of the middle- and long-wavelength-sensitive cones derived from measurements in observers of known genotype. Vision Research, 40(13), 1711–1737. https://doi.org/10.1016/s0042-6989
- Stockman, A., Sharpe, L. T., & Fach, C. (1999). The spectral sensitivity of the human short-wavelength sensitive cones derived from thresholds and color matches. *Vision research*, 39(17), 2901–2927. https://doi.org/10.1016/S0042-6989(98)00225-9
- Taveras-Cruz, Y., He, J., & Eskew, R. T., Jr. (2022). Visual psychophysics: Luminance and color. Progress in Brain Research, 273(1), 231–256. https://doi.org/10.1016/bs.phr.2022.04.004
- Wang, Q., Richters, D. P., & Eskew, R. T., Jr. (2014). Noise masking of S-cone increments and decrements. *Journal of Vision*, 14(13), 8. https://doi.org/10.1167/14.13.8
- Watson, A. B. (1986). Temporal Sensitivity. In K. R. Boff, L. Kaufman, & J. P. Thomas (Eds.), Handbook of perception and human performance (Vol. 1: Sensory processes and perception). NY: Wiley.
- Wuerger, S., Ashraf, M., Kim, M., Martinovic, J., Perez-Ortiz, M., & Mantiuk, R. K. (2020). Spatio-chromatic contrast sensitivity under mesopic and photopic light levels. *Journal of Vision*, 20(4), 23. https://doi.org/10.1167/jov.20.4.23
- Zhou, H., Friedman, H. S., & von der Heydt, R. (2000). Coding of border ownership in monkey visual cortex. *The Journal of Neuroscience*, 20(17), 6594–6611. https://doi. org/10.1523/JNEUROSCI.20-17-06594.2000